MEASUREMENT AND EVALUATION OF SWIRL-TYPE FLOW IN LABYRINTH SEALS OF CONVENTIONAL TURBINE STAGES

L. Hauck
Institut für Thermische Kraftanlagen
Technische Universität München
8000 München 2, Federal Republic of Germany

SUMMARY

Previous studies of rotor whirl instability pointed out two different mechanisms inducing lateral forces within non-contacting labyrinth-type seals. Evaluating the part of exciting forces that results from leakage losses is possible by means of variable flow contraction in the gap of a seal with variable clearance at the circumference. The dominating part of exciting forces has its origin in unequal pressure distributions at the circumference of the seal with a shaft in out-of-centre position. The pressure distribution is mainly influenced by swirl-type flow at seal entry.

The installation of a computer controlled cantilevered pitot cylindre within the seals of two different test stages enables the measurement of flow conditions within every cavity of the labyrinth. The effects of load factor and rotor eccentricity were determined on flow conditions in test series for both stages. The results indicate that swirl-type entry flow follows the rules of potential swirl. Within the labyrinth cavities two spatial separated flow areas are to consider. A dominating flow in peripheral direction nearly fills the space between the sealing strips and the ceiling of the cavity. Below this flow, an area of axial mass transport is situated, with a slight peripheral component, limited on the nearest surroundings of the seals gap and the rotor surface. Between both flows, an exchange of energy takes place. Within the gaps, flow direction depends on axial velocity and therefore on variable flow contraction. A balance of energy within the seal and the cavities interprets the results of lateral force measurements as an influence of friction at the sealing strips surface and the rotating shaft surface. Stages with their blades put together in buckets by means of shrouding segments are particularly influenced by the rotating speed of the shrouding.

One method to describe the flow conditions more closely is dividing the leakage flow in stream tubes with varying cross sections at the circumference. This enables a one-dimensional view on the flow along every stream tube. Additionally, two flow areas within every cavity must be taken into account. Therefore, the local profile of the tube is unequal to the geometric boundary of the labyrinth. Other effects, as rotating shaft, flow contraction and compressible flow through the labyrinth may be considered as well.

INTRODUCTION

Non-contacting seals are already known as a possible reason of self-excited rotor vibrations in turbomachinery. A large number of papers (ref. 1,2,3,4), based on theoretical approaches and experimental results, pointed out two different mechanisms as origin of exciting lateral forces.

Exciting Forces due to Leakage Losses

A change of leakage losses at the circumference, caused by the variable gap resulting from rotor eccentricity, leads to a change of blade force at the circumference (ref. 1). The resultant exciting force is given by the integral of local blade force dU at the circumference

$$Q_2^S = \int_0^{2\pi} dU \cos\varphi = -\frac{U_{is}}{2\pi} \int_0^{2\pi} \xi_{sp}(\varphi) \cos\varphi \, d\varphi \qquad (1)$$

where φ is the circumference angle. Following equation (1) tangential forces can be expressed by isentropic tangential force U_{is} and the leakage loss ξ_{sp}. The leakage loss is determined by the geometric boundary of the seal and the performance of the stage at a certain operating point. This is taken into account by the constant factor C.

$$\xi_{sp} = C \alpha s \qquad (2)$$

Additional, the leakage losses depend on local clearance s and the flow contraction factor α. Both change at the circumference.

While geometric clearance can be easily put up, the determination of varialbe flow contraction is still difficult. Therefore, flow contraction is set up as a global constant factor α^* applying to centric rotor position. Flow contraction causes a higher uniformity of gap clearance at the circumference with a rotor in out-of-centre position. This is considered by the effective eccentricity e_{eff}.

$$e_{eff} = v_F e \qquad (3)$$

The uniformity factor v_F (ref. 5) is put up using flow contraction in the narrowest and the widest gap.

$$v_F = (\alpha_{0°} s_{0°} - \alpha_{180°} s_{180°})/(2e) \qquad (4)$$

According to these relations, exciting force can be calculated by using the isentropic tangential force, the eccentricity, the uniformity factor and the flow contraction.

$$Q_2^S = -\frac{U_{is}}{2} C\alpha^* v_F e \qquad (5)$$

Exciting Forces due to Pressure Distribution

If fluid flow through the labyrinth is superimposed by a peripheral flow component, a dominating lateral force arises from the pressure distribution in shrouded stages (ref. 3,6,7,8). With dp for the local pressure, z the coordinate in axial direction and b the width of the shrouding, the exciting force is given by

$$Q_2^D = -\int_0^b\int^{2\pi} dp \sin\varphi = -\int_0^b\int_0^{2\pi} p(z,\varphi) \sin\varphi \, r \, d\varphi \, dz \qquad (6)$$

Calculating the pressure distribution is problematic, since the location of maximum pressure depends on swirl-type flow at seal entry. A complete solution, like in the case of leakage losses, is not yet possible.

DESCRIPTION OF TEST APPARATUS

Investigated Stages

The flow patterns within the labyrinth seals of two test stages were measured, to check existend methods of calculation and set up better resolutions of calculating exciting forces.

Figure 1 shows the investigated turbine stages. The stage marked with the number I is a reaction type stage. As may be seen from the blades profile, stage II is a impulse type one. Besides this, the shrouding of stage II is closed, while the blades of stage I are put together in buckets of three or four blades. Further data of the investigated stages are gathered in table 1. Both stages have stepped seals that are similar in its geometric shape.

Distribution of Measuring Positions

Figure 2 shows the labyrinth seal of one stage. The cantilevered pitot cylindre illustrated in the figure was used for flow measurements. The revolving cylindre drive was fixed in ball-bearings and designed to measure flow patterns in every cavity of the labyrinth seal. The structure of the drive can be seen in figure 3. The gear box includes two different drives. Revolving the cylindre is done by drive (c), while drive (d) moves the cantilevered pitot cylindre to its axial position. Moving from one cavity to the next is done by drive (a). Before revolving the gear box, the pitot cylindre must be lowered into the box. Then the whole drive is raised by three pneumatic motors, revolved by drive (a) to the next position and moved back by the pneumatic motors.

In this way, a net of measuring positions is distributed over a sectional area in the seal. Figure 4 shows the position of the measuring points within the seal. Several eccentric positions of the rotor could be adjusted at the inves-

tigated stages. The resulting variable gap clearance at the circumference influences the number of measuring positions. The whole net of measuring positions can be divided in two areas as shown in picture 4. Those positions, that are located within the cavity are used for all measurements. Previous studies supposed a fundamental influence of flow in the clearance on the whole flow patterns in the seal. Therefore, additional measuring positions were provided in the surroundings of every throttle gap. The number of positions depends on the adjusted eccentricity. The geometric clearance varies between 0,1 and 0,7 mm (0,004 and 0,027 inch). To enable the measurement of flow conditions as exact as possible, measuring positions were distributed over the clearance with a distance of 0,1 mm (0,004 inch) from each other.

Cantilevered Pitot Cylindre

As already mentioned, a cantilevered pitot cylindre was used for the measurements of flow conditions. The cylindres diameter is 1 mm (0,039 inch), that of the measuring hole is 0,1 mm (0,004 inch). Figure 5 shows the structure of the measuring unit. It consists of the pitot cylindre, a miniature pressure transducer and the cylindre carrier. Measurement is done by revolving the cylindre and picking up pressure data simultaneously. The position and the level of the total pressure in the stagnation point, as well as the static pressure at the measuring position is obtained from the pressure distribution. Thus, intensity and direction of flow velocity can be derived in an area perpendicular to the cylindre.

Test results may be influenced by a wall close to the cylindre. Therefore, tests were made in a special prepared wind tunnel. Deviations of the results due to a nearby wall have been taken into account. The whole test apparatus was controlled and watched by a desktop computer. In addition, this computer gathered test and position data.

IMPULSE TYPE STAGE

The result of a test period can be seen in figure 6 with the rotor in centric position. The figure shows the measured vectors of flow velocity in each position, described by arrows. Measuring areas are illustrated by dashed linies in the labyrinth scheme. The arrows length shows the level of velocities. Its direction is equivalent to the flow direction of the measured cylindre flow. The entry flow into the first cavity follows the rules of potential swirl.

Spatial Distribution of Velocity

Figure 7 shows the spatial distribution of flow velocities in a qualitative illustration. As shown in the figure, a dominating flow in peripheral direction fills the labyrinth cavities. This core flow is overlapped by a heavy, screw-like flow near the walls of the labyrinth. The three dimensional distribution of the flow velocity is determined by measurements over the height of the cavity, because only two dimensional velocities are measured

by the pitot cylindre. The directions of flow velocity near the ceiling of the cavity and the rotors surface, together with the rules of mass continuity point out a "vortex-screw" rotating with high peripheral velocity within the cavity. The rotating direction of the vortex is determined by the leakage flow and the geometric boundary of the cavity. In the second cavity of a stepped seal, as illustrated in the figure, the leakage flow dashes against the step of the shrouding. The flow is turned round at this point and raises, until it touches the ceiling of the cavity. The "vortex-screw" revolves counter clockwise due to the additional pressure drop to the next cavity. Caused by the set-back of the shrouding in the third cavity, the expansion of the leakage flow is limited on the nearest surroundings of the rotor surface. Above this flow, a dominating tangential flow nearly fills the space between the sealing strips and the ceiling of the cavity. A "vortex-screw" revolving clockwise in this cavity, grows by jet mixing and impulse exchange.

Axial Flow in the cavities

Figure 8 shows the distribution of axial velocities in the cavities of the labyrinth. Measurements were made near the ceiling, in the middle of the cavity and at the shrouding by changing the eccentricity of the rotor. Up stream velocities are marked by negative axial flow components. They are caused by "vortex-screws". The rotating direction of the vortex is determined by velocity near the shrouding and the ceiling of the cavity. The influence of rotor eccentricity on flow patterns in this region is unimportant.

Velocities at the Gap Clearance

Near the gap clearance, velocity distribution depends hard on rotor eccentricity. Especially the distribution of axial velocities along the clearance is modified, while tangential velocity is not influenced by rotor position. Figure 9 shows the distribution of axial velocity and flow angle in the gap clearance. The first measuring position is not situated within the clearance, because a minimum distance to the rotating surface must be regarded to secure the pitot cylindre. For the same reason, the velocity close to the shrouding could not be measured. The influence of the seal clearance on the velocity can be seen in the figure. Additional the security distance to the cylindre is shown, with a rotor that is 0,3 mm (0,012 inch) out of centre. The velocity distribution in the smallest clearance, according to e = - 0,2 mm (0,008 inch), changes continuously with increasing clearance. This points out the influence of varying flow contraction. The flow angles, an important factor of calculation, are shown in the lower figure. As already mentioned, tangential flow does not change by eccentricity. Therefore, flow angles are essential determined by axial velocity and can be evaluated using leakage flow and flow contraction.

Exitation Coefficient of Impulse Type Stage

Exciting forces can be defined as dimensionless coefficient too.

$$K2 = K_2^D + K_2^S = \frac{Q_2^D/U_{is}}{e/l''} + \frac{Q_2^S/U_{is}}{e/l''} \qquad (7)$$

The exitation coefficient K2 is given by the quotient of related exciting force Q/U_{is} and relative eccentricity e/1", where 1" is the length of the rotor blade.

In figure 10, this coefficient is plotted over the power of the stage, represented by the load factor $\Psi = 2\Delta h_{is}/u^2$, with Δh_{is} as the isentropic enthalpy difference and u the circumferential speed. The resulting force on the rotor of impulse-type stage is illustrated in curve (a). Forces due to pressure distributon and to leakage losses are both included. The exitation coefficient induced by pressure distribution was measured and is shown in curve (b). The part of leakage losses cannot be measured directly. Therefore, curve (c) shows the calculated exitation coefficent of leakage losses. Near load factor 3.5, a remarkable behaviour of excitation coefficient can be seen. A close examination of this behaviour points out that the speed of rotation is equal to the peripheral flow at labyrinth entry. Beyond this point, velocities of labyrinth flow and the speed of rotation are different. Thus, the course of exitation coefficient can be explained as influence of shrouding friction. This effect has not yet been regarded as important, especially for seals with short axial length.

Balance of Energy

Based on the results of measurements, a balance of energy within the seal and the cavities is set up. Figure 11 illustrates this balance of energy for different operating points of the impulse type stage. A clear supply of energy by the shrouding can be seen at load factor 2 and 3, whereas elimination of energy dominates at load factor 4. Calculating the losses as well as the velocities and the pressure in the cavities, enables the evaluation of energy flow. Friction losses can be determined from the mass flow of the "vortex-screw" and the pressure drop caused by friction. The distribution of energy losses in the cavities and the shrouding, shown in the picture, base on this evaluation.

REACTION TYPE STAGE

The energy supply of the labyrinth is influenced by the construction of the shrouding. The blades of reaction type stage are put together in buckets of three or four blades by means of shrouding segments that are separated from each other by a gap.

Figure 12 shows the flow pattern within the labyrinth seal of this stage. Because of the similar geometric shape the flow in this seal can be compared with stage II. A dominating tangential flow overlapped by a "vortex-screw" results as well. But it is additionally influenced by a jet flow that injects perpendicular to the shrouding. This jet flow reaches to the ceiling of the cavity and causes pressure oscillations picked up during additional measurements. The oscillations at high frequency level do not influence the force due to pressure distribution directly, but the jet flow, injected from the gaps of the shrouding, works like a rotating blade. Thus the swirl of flow in the cavities is influenced.

Exitation Coefficient of the Reaction Type Stage

As the jet flow depends on the rotating speed of the shrouding, the influence of shrouding velocity on exciting forces increases. In figure 13, the exitation coefficient is plotted over the load factor of the reaction type stage. Because of the slight entry swirl, exitation coefficients are generally lower. In spite of this, a heavy influence of shrouding velocity on measured resulting exitation is to be seen. Near load factor four, the measured tangential flow is equal to the rotating speed of the shrouding. The lowest exitation coefficient is measured at this load. Obviously, the injection flow is able to accelerate the swirl of entry flow in a way, that raises the exciting forces by lowering power. At high load factors, influence of injection flow on entry swirl prevents an increase of exitation with the load number.

CONCLUDING REMARKS

As shown by the results of investigations, high tangential velocities, varying flow contraction together with its influence on flow angles, and the effect of friction on the shrouding are to be especially considered by the calculation of exciting forces. A method that considers these influences is given by ref (9). In this case, the labyrinth flow is described by dividing the leakage flow in stream tubes that are joint against one another at the circumference.

The shape of a stream tube is principally illustrated in figure 14. At every cross section, the equations of impulse and energy are resolved iteratively, using the continuity of mass flow. A part of the working fluid is branched at the entry of the seal. The shape of the stream tubes within the seal depends on various conditions. The leakage flow is added to the working fluid at outlet of the seal. This kind of view gives a description of complete flow patterns, as usually present in labyrinth seals, by means of a one-dimensional flow.

The test results enable an extension of this method. Two different flow areas, relating to the flow within the cavity and the leakage flow are to consider. New statements are needed to describe the local profile of the stream tubes that are not identical with the geometric boundary of the labyrinth. Additionally, the influence of shrouding velocity must be considered by friction and velocity at the rotor surface. Besides this, the change of flow angles due to flow contraction is important. Because of a slight pressure drop within every cavity, calculation in the cavity can be done using the rules of incompressible flow. The pressure drop from one cavity to the next however must be considered. Therefore, compressible flow should be supposed for calculations in the gap. Using these additional considerations, the accuracy of this method would raise essentially. Actual work is done on this topic and will be described in a later paper.

REFERENCES

1. Thomas, H.-J.: Instabile Eigenschwingungen von Turbinenläufern, angefacht durch die Spaltenströmung in Stopfbuchsen und Beschaufelungen. Bull. de L`AIM (1958) Nr. 11/12, S. 1039-1063

2. Alford, J. S.: Protecting Turbomachinery From Selfexited Whirl. Jornal of Engineering for Power, Trans. ASME, Series A, 38 (1965) pp333-344

3. Lomakin, A. A.: Die Berechnung der kritischen Drehzahl und der Bedingung für Sicherung der dynamischen Stabilität des Läufers von hydraulischen Hochdruck-Maschinen unter Berücksichtigung der Kräfte, die in den Dichtungen entstehen. Energomasinostroenie 4 (1958) H. 4, S. 1-5

4. Thomas, H.-J.: Urlichs, K.; Wohlrab, R.: Läuferinstabilität bei thermischen Turbomaschinen infolge Spalterregung. VGB Kraftwerkstechnik 56 (1976) H. 6, S. 377-383

5. Hauck, L.: Vergleich gebräuchlicher Turbinenstufen hinsichtlich des Auftretens spaltströmungsbedingter Kräfte. Konstruktion 33, (1981) H. 2, S. 59-64

6. Childs, D. W.: Dressman, J. B.: Testing of Turbulent Seals for Rotordynamic Coefficient. NASA Publication 2133, May 1980

7. Benckert, H.; Wachter, J.: Flow Induced Coefficients of Labyrinth Seals for Application in Rotordynamics. NASA Conference Publication 2133, (1980)

8. Jenny, R.: Labyrinthe als Ursache selbsterregter Rotor-Schwingungen bei Radialverdichtern. Technische Rundschau Sulzer (1980) H. 4, S. 149-156

9. Urlichs, K.: Durch Spaltströmungen hervorgerufene Querkräfte an den Läufern thermischer Turbomaschinen, Diss. TU München 1975; s.a. Ing.-Arch. 45 (1976) H.3, S. 193-208

TABLE I. - DATA OF INVESTIGATED STAGES

		stage I	stage II
Speed	min^{-1}	4000	5000
Diameter of stage	mm	420	420
Number of blades			
nozzle vanes		50	63
wheel blades		50	99
Length of blades			
nozzle vanes	mm	40.6	38.6
wheel blades	mm	42.0	40.0
Flow angles			
α_1	degrees	17.3	12.9
β_2	degrees	17.3	20.1
Clearance			
nozzle vanes	mm	0.48	0.40
wheel blades	mm	0.43	0.40
Width of shrouding			
nozzle vanes	mm	22.4	36.0
wheel blades	mm	19.0	27.0
Degree of reaction		0.45	0.20

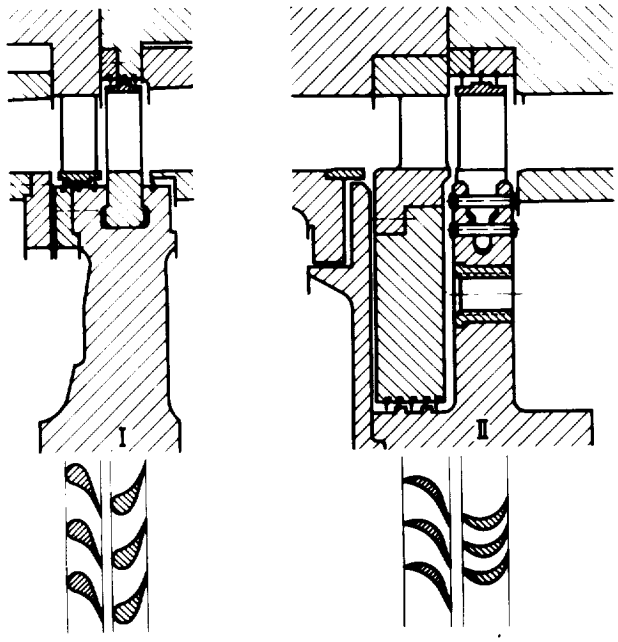

Figure 1. - Investigated stages.

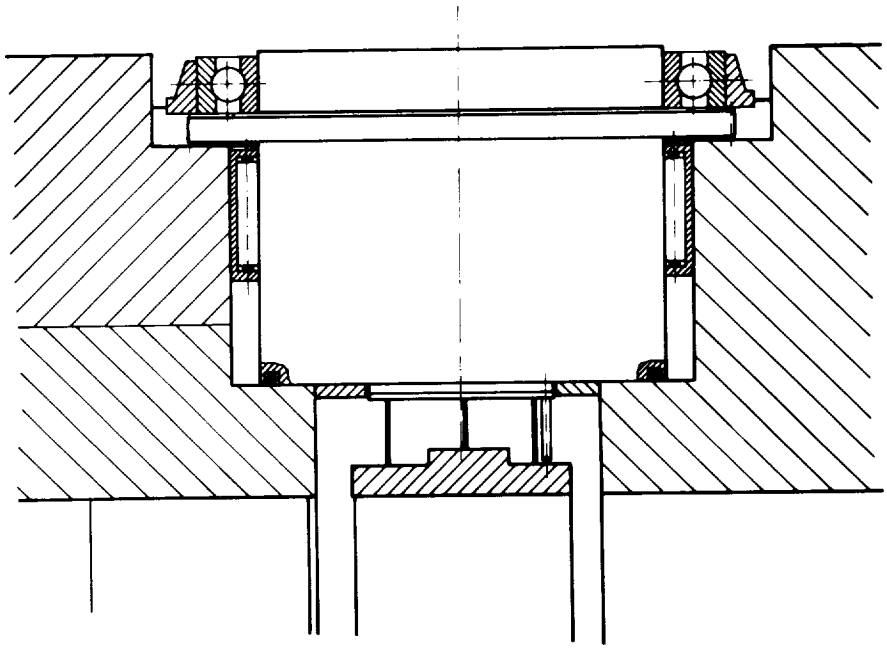

Figure 2. - Labyrinth seal and measuring unit.

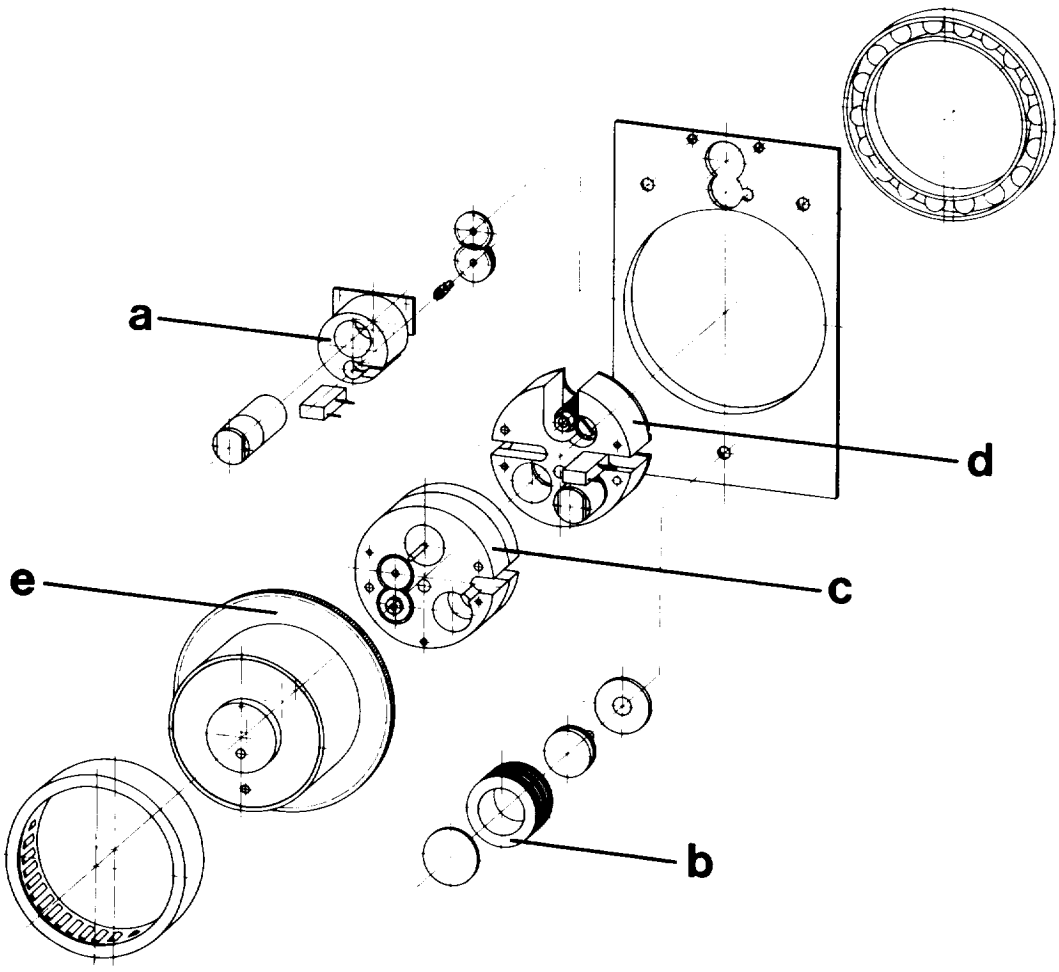

a revolving drive
b pneumatic motor
c revolving drive
d axial moving drive
e housing

Figure 3. - Structure of the gear box.

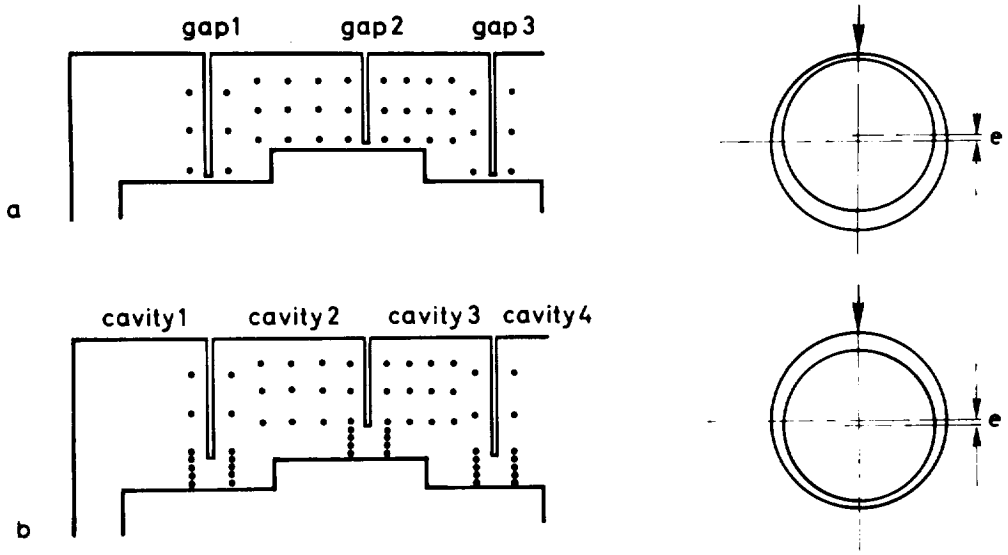

a smallest clearance
b widest clearance

Figure 4. - Distribution of measuring positions.

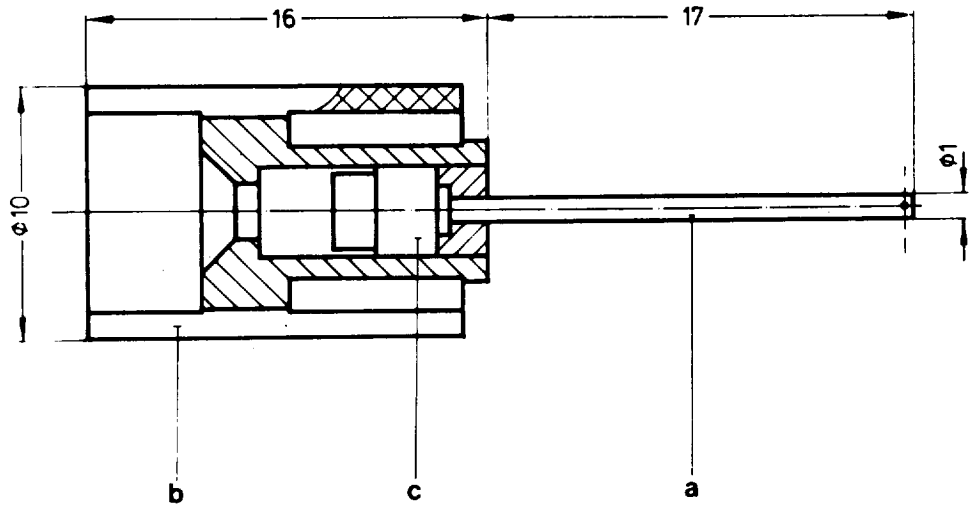

a pitot cylindre
b cylindre carrier
c pressure transducer

Figure 5. - Structure of the measuring unit.

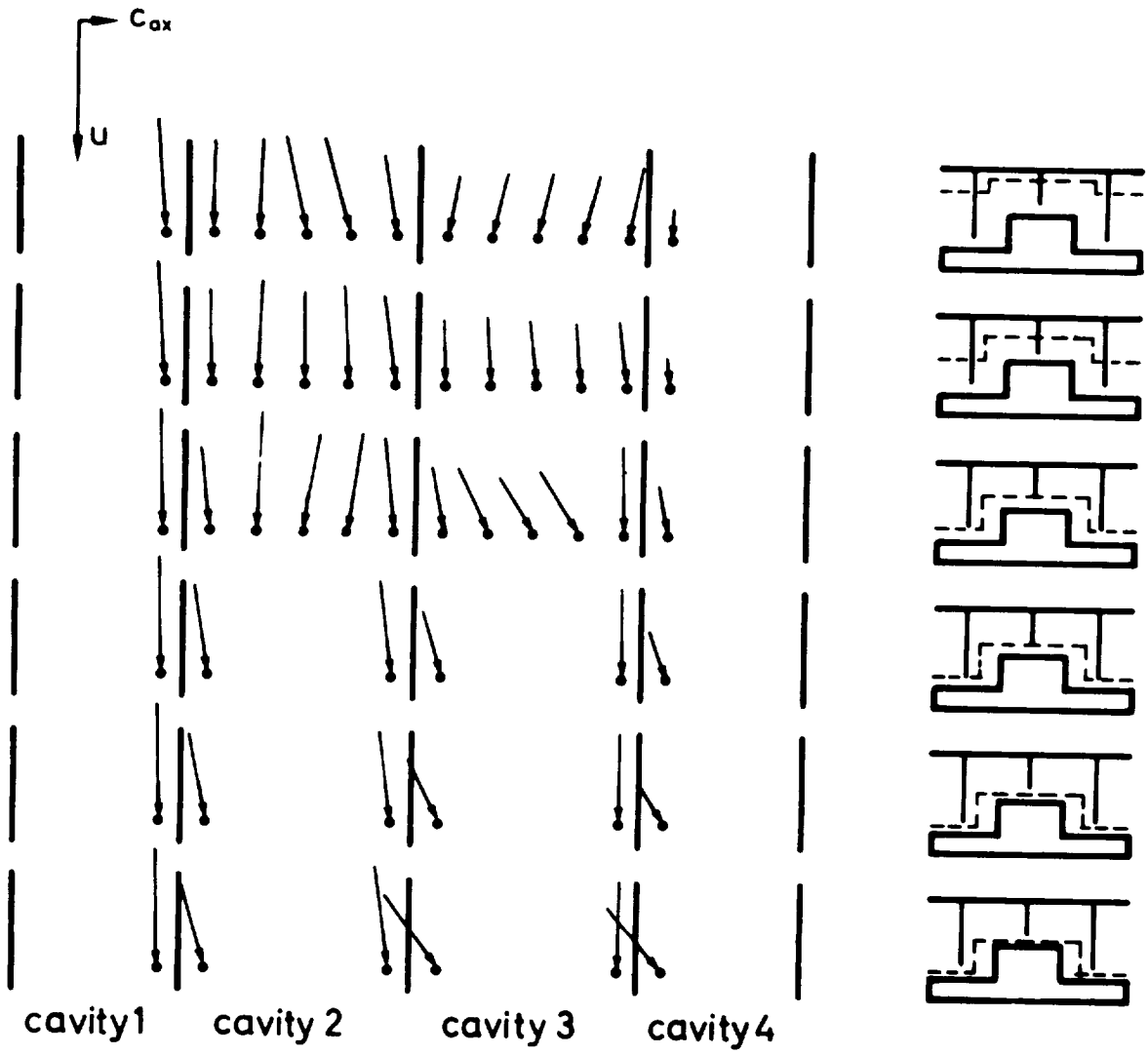

Figure 6. - Flow velocity within the cavities (measured).

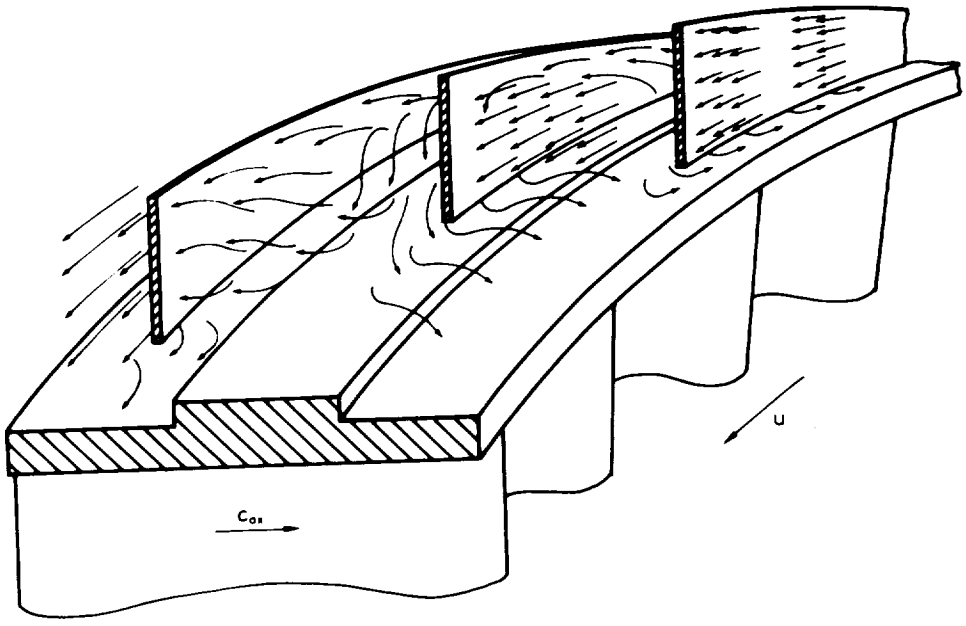

Figure 7. - Spatial distribution of flow velocities (stage II).

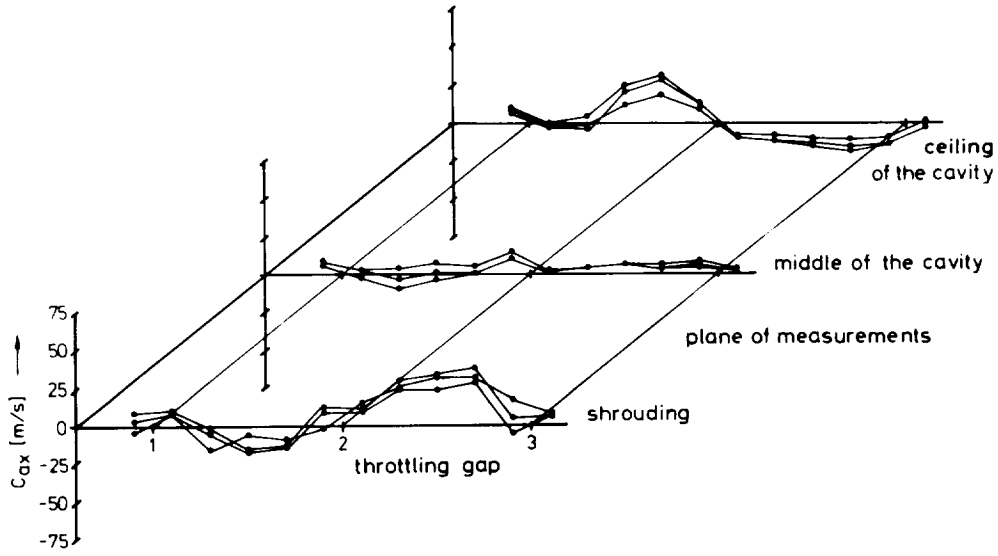

Figure 8. - Distribution of axial velocity in the cavities (measured).

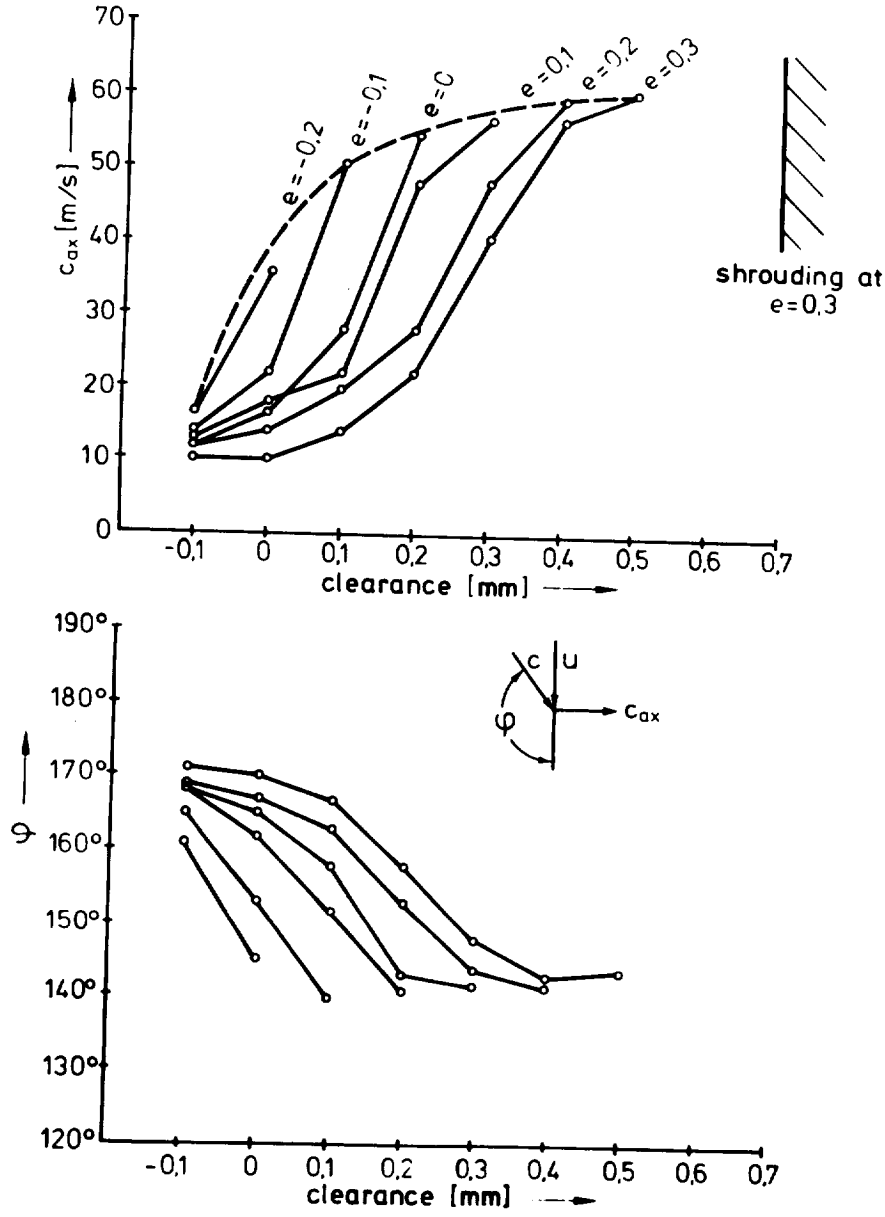

Figure 9. - Axial velocity and flow angle in the gap (measured).

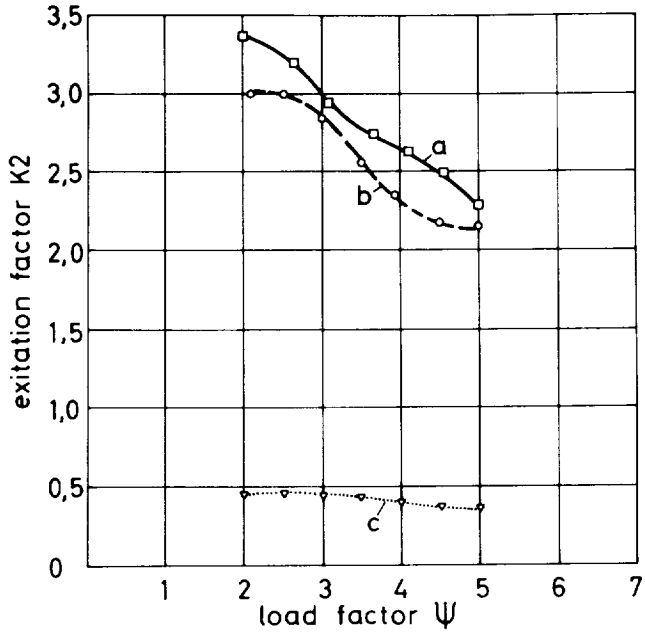

a resulting exitation (measured)
b exitation by pressure distribution (measured)
c exitation by leakage losses (calculated)

Figure 10. - Exitation factor and load factor (stage II).

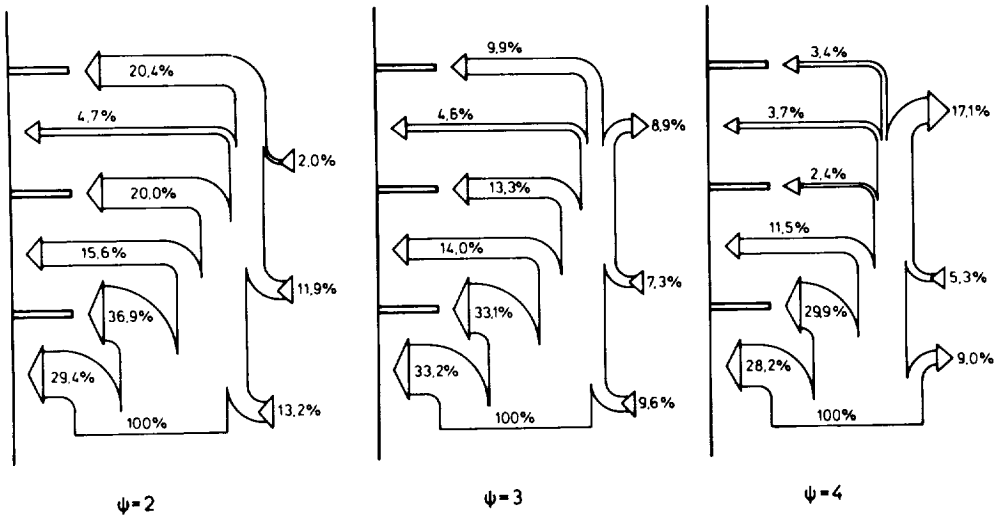

Figure 11. - Balance of energy and load factor (stage II).

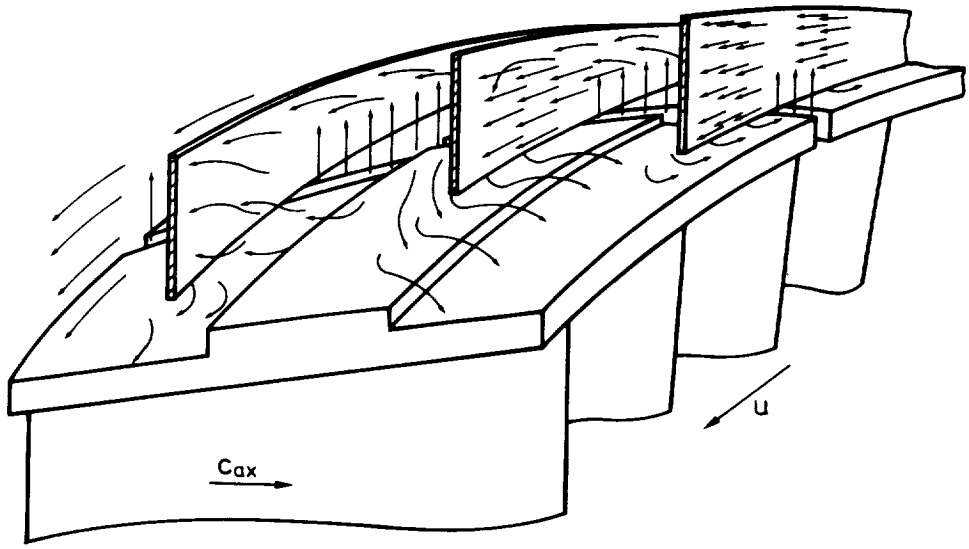

Figure 12. - Spatial distribution of flow velocities (stage I).

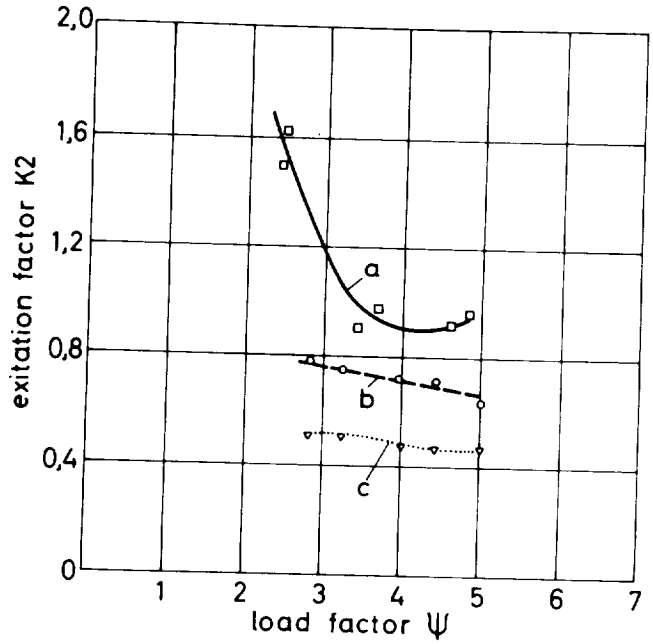

a resulting exitation (measured)
b exitation by pressure distribution (measured)
c exitation by leakage losses (calculated)

Figure 13. - Exitation factor and load factor (stage I).

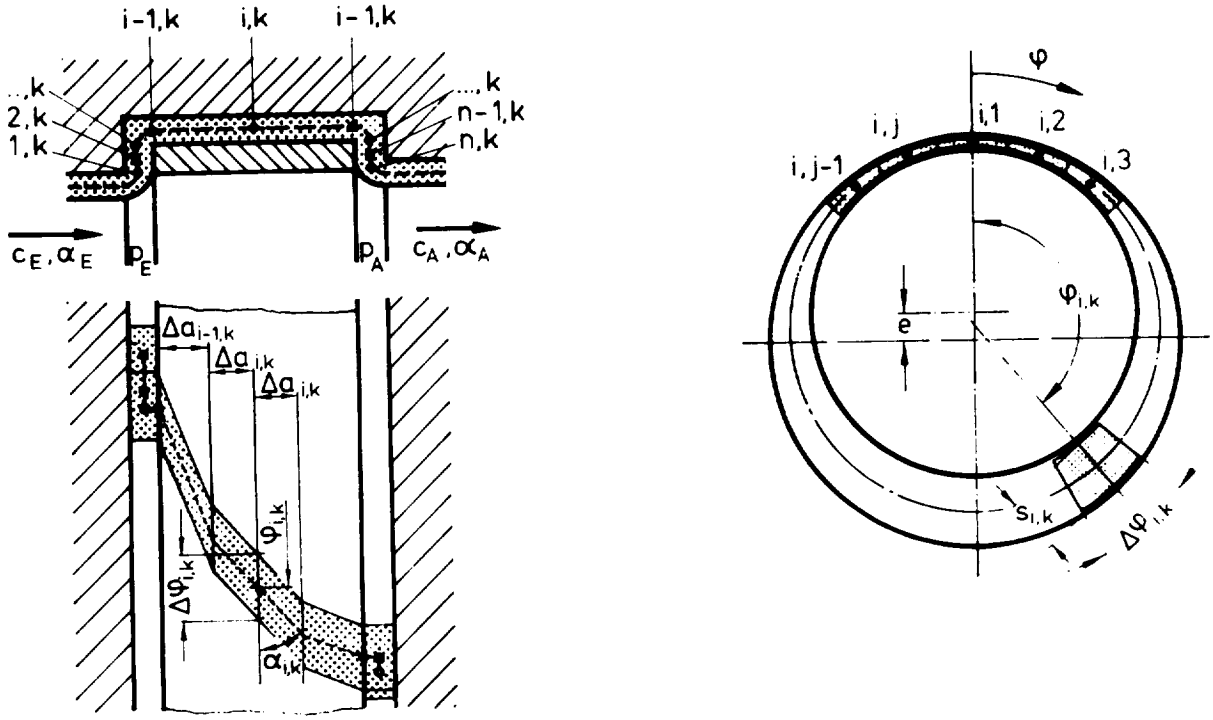

Figure 14. - Shape of stream tube.